Hybrid Loss-Compensated Plasmonic Device

Hosseini Alast, Fatemeh; Nikkhah, Mohsen; Li, Xiao; NG, Tsz Fai Jack; Ghasemi, Amirhossein B.; Latifi, Hamid; CHEAH, Kok Wai

Published in:
Advanced Optical Materials

DOI:
10.1002/adom.201801189

Published: 05/03/2019

Hybrid Loss-compensated Plasmonic Device

Fatemeh Hosseini Alast, Mohsen Nikkhah, Xiao Li, Jack Ng,

Amirhossein B. Ghasemi, Hamid Latifi and K. W. Cheah*

Abstract: Abstract: We studied how active medium affects the Rabi-analogue splitting when an active plasmonic microcavity mode is coupled to a surface plasmon polariton mode. The incorporation of Rubrene-like molecules in the plasmonic microcavity resulted in stronger modal coupling. Anti-crossing was observed with a large Rabi-analogue splitting energy of 280 meV in the strong coupling regime. The active medium contributed to the split enhancement through channeling more energy towards the coupling. The variation of photoluminescence emission and exciton-cavity mode coupling from the hybrid plasmonic microcavity were also measured. This work shows that by introducing an active medium in the microcavity, mode coupling between microcavity and surface plasmon polariton can be enhanced and the hybrid plasmonic device exhibits parity time symmetry characteristics.

Dr. F. H. Alast[1, 2], M. Nikkhah[2], X. Li[1], Dr. J. Ng[1], Dr. A. B. Ghasemi[2], Prof. H. Latifi[2], Prof. K. W. Cheah[1]

[1]Department of Physics, Institute of Advanced Materials, and Institute of Computational and Theoretical Studies, Hong Kong Baptist University, Kowloon Tong, Hong Kong, China

[2]Department of Physics, Shahid Beheshti University, G.C. Evin, Tehran, Iran.

E-mail: kwcheah@hkbu.edu.hk

1. Introduction

The strong coupling regime was analyzed by many research groups in different hybrid plasmonic-organic/inorganic frameworks [1]. Hence the modal coupling of hybrid plasmonic cavity was abundantly studied. The cavity mode and Surface Plasmon Polariton (SPP)

coupling produces Rabi-analogue splitting similar to that of quantum electrodynamic phenomenon where a single emitter interacts with the resonant field of the resonator [2]. The modal splitting occurs when two modes of the same energy, and thus same frequency, are coupled. It is an acknowledged fitting and controlling energy distribution or exchange pathway to control device characteristics in the strong coupling regime [3].

Furthermore optoelectronic devices have gradually replaced conventional optical and electrical devices in many applications. Thus it is essential to improve fabrication techniques and extend exerted material to get optimum performance beside cost-effective of mass production. For plasmonic-based optoelectronic devices, the interaction of dielectric and conductor in them are essential to explore the plasmonic behavior at various interfaces. Dielectric can be as inorganic and organic; its selection depends on their attributes. Presently organic materials are particularly attractive due to their long exciton lifetime which makes strong modal coupling in interaction with surface plasmon polaritons (SPP) probable [4]. To achieve strong coupling, organic material ought to possess limited transition linewidth [5] like using J-aggregate molecules at plasmonic interfaces [6]. But J-aggregate molecules require special environmental prerequisites to function properly and maintain stable interaction. In this study, we used small florescent molecule to investigate the strong modal coupling at the organic/plasmonic interface. We focus on the strong modal coupling of plasmonic microcavity using florescent organic material, EY51 (Rubrene-like), in dielectric medium of plasmonic microcavity. The introduction of an active medium has effectively introduce a loss-compensated channel in the microcavity. We believe the interaction of active medium cavity and plasmonic nanostructure has generated a new plasmonic system that can open up a new degree to control modal coupling, analoguous to the modal coupling control in parity time symmetry system; we observed anti-crossing with large Rabi-analogue splitting at cavity mode-SPP coupling in large area hybrid plasmonic microcavity. We also investigated the luminescence intensity which acts as loss-compensation impact on the coupling strength of cavity. In addition, the photoluminescence (PL) emission measurement was carried out for

plasmonic and photonic microcavity which acquired higher intensity of PL emission in the plasmonic cavity than that of photonic. The device was fabricated with conventional photolithography to provide the required practicality and cost-efficiency of mass production for various applications [7].

2. Theory

The light-matter interaction at the plasmonic microcavity can be broadly described by the following Hamiltonian [8]:

$$H = \begin{bmatrix} \omega_{cav} + i\Gamma_{cav} & g \\ g & \omega_{spp} + i\Gamma_{spp} \end{bmatrix} \tag{1}$$

where ω_{cav} and ω_{spp} are, respectively, the resonant frequencies of the cavity mode and SPP mode, Γ_{cav} and Γ_{spp} represent the corresponding loss, and g represents the modal coupling. The resonant frequencies of the coupled modes can be obtained by diagonalizing equation (1):

$$\begin{aligned} \omega_{\pm} &= \frac{1}{2}\left[\left(\omega_{cav} + \omega_{spp}\right) + i\left(\Gamma_{cav} + \Gamma_{spp}\right) \pm \sqrt{4g^2 + \Delta\omega^2 - \Delta\Gamma^2 + 2i\Delta\Gamma\Delta\omega}\right] \\ &= \frac{1}{2}\left[\left(\omega_{cav} + \omega_{spp}\right) + i\left(\Gamma_{cav} + \Gamma_{spp}\right) \pm \sqrt{A + iB}\right] \end{aligned} \tag{2}$$

where $A = 4g^2 + \Delta\omega^2 - \Delta\Gamma^2$ and $B = 2\Delta\Gamma\Delta\omega$, $\Delta\Gamma = \Gamma_{cav} - \Gamma_{spp}$, and $\boldsymbol{\Delta\omega = \omega_{cav} - \omega_{spp}}$.

From equation (1), one can rewrite the ratio of splitting to the resonant linewidth:

$$\gamma = \frac{\mathrm{Re}\{\omega_+\} - \mathrm{Re}\{\omega_-\}}{\mathrm{Im}\{\omega_+\} + \mathrm{Im}\{\omega_-\}} = \frac{\omega_+ - \omega_-}{\Gamma_{cav} + \Gamma_{spp}} = \frac{\sqrt{2}\sqrt{A + \sqrt{A^2 + B^2}}}{\Gamma_{cav} + \Gamma_{spp}} \tag{3}$$

For large γ, one can easily observe the modal splitting, whereas for small γ, the splitting only occurs for narrow linewidth. It is reasonable to assume that Γ_{cav} and Γ_{spp} for each system will not change. Then larger *A* and *B* will lead to larger γ, and thus larger splitting.

We note that a large *g* (coupling) and $\Delta\omega$ will certainly increase γ, whereas a larger $\Delta\Gamma$ will increase *B* but decrease *A*, and therefore it may not increase γ. Here we note that at the special case of $\Delta\omega = 0$, then *B*=0. Accordingly, decrease in $\Delta\Gamma$ may lead to increase in splitting if $|\Delta\Gamma| < |2g|$. In this aspect, the active medium in the hybrid plasmonic microcavity could contribute to the strong coupling of SPP and cavity mode under the four-wave mixing framework.

3. Device Fabrication

We used conventional photolithography technique to fabricate the large area plasmonic nanostructure [9]. The ruled grating pattern was fabricated on glass substrate in large area (10×10 mm^2); it can be extended to several centimeters by using proper expanding/collimating setup. The pitch size of grating is 360 nm with a height of 20 nm. Scanning electron microscopy (SEM) was used to determine the surface quality and uniformity of fabricated grating pattern, as shown in figure (1). The interference pattern was generated by He-Cd laser beam with wavelength of 442 nm upon the spin-coated thin film of positive photoresist (PR) (AP-R 5300). Subsequently, we integrated the ruled metal grating into photonic cavity to form hybrid plasmonic microcavity. The silver layers with 45 nm and 120 nm thicknesses were thermally evaporated as front and back mirrors of photonic cavity, respectively. The intermediate dielectric layer of cavity is a thin film of EY51 (diluted with toluene in 0.5 mg/ml) deposited on front mirror and followed by PMMA (polymethyl methacrylate) layer (diluted with chlorobenzene in ratio of 1:1); both dielectric layers were spin-coated. The luminescent intensity of EY51 is adjusted through varying its concentration and in order to maintain the same cavity modes, the total dielectric thickness was adjusted so that it has the same effective refractive index. Figure (1) shows the device configuration.

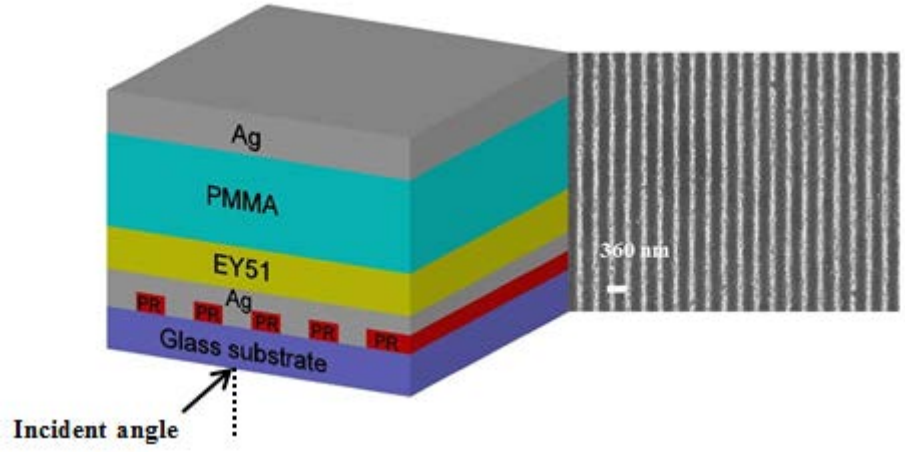

Figure 1. The hybrid plasmonic microcavity configuration and the SEM image of grating surface quality.

4. Results and Discussion

The TM (Transverse Magnetic) reflected mode was measured to evaluate cavity mode-SPP coupling at the interface. The results show that an extremely strong cavity mode-SPP coupling at the incident angle of 50 degrees and this is obtained with the fabricated plasmonic microcavity with dielectric medium thickness of 630 nm and the EY51 molecule coated thickness is roughly 30 nm, (cavity (a)). Anti-crossing has resulted in a large Rabi-analogue splitting around common resonance wavelength, 619 nm, of the two coupled modes. The splitting energy is 280 meV (85 nm linewidth), (figure (2a)). In comparison with the passive plasmonic microcavities [8] in which the splitting energy is only 70 meV, using fluorescent material film resulted in a considerable improvement of the coupling quality and strength and created a larger modal splitting on the coupled system.

In order to elucidate the role of EY51 on the coupling strength, two more hybrid plasmonic microcavities with cavity dielectric medium of 600 nm and 670 nm thick were fabricated; the thicknesses of fluorescent material are 50 nm and 80 nm, respectively. The results show that there is an optimum EY51 film thickness giving the strongest coupling strength of the hybrid plasmonic systems. Anti-crossing occurred with splitting energy at 240 meV for the cavity

with 50 nm fluorescent film (cavity (b)), figure (2b), and there is no coupling for cavity with 80 nm florescent film (cavity (c)), figure (2c). Hence, the exchange energy between the coupled modes is present in cavities (a) and (b) while it does not exist in the cavity (c). The exchange energy of the coupled system aroused from the coupling of cavity mode and SPP mode and thus the coupled system involves two modes with narrow linewidth and strong local field ($\Delta\lambda_{LP\ mode}$ = 15 nm , $\Delta\lambda_{UP\ mode}$ = 13 nm) compared with the uncoupled system ($\Delta\lambda_{cav}$= 16 nm , $\Delta\lambda_{spp}$= 66 nm). Figure (2d) compares the experimental (cavity (b)) and simulation results. The simulations are carried out using the commercial finite element method package COMSOL Multiphysics using the periodic boundary conditions. Clearly, the reflection dips from experiments and simulation agree with each other well.

We studied the angular dispersion of modal coupling by varying incident angle from 48 to 52 degrees at the hybrid plasmonic microcavities (a), (b) and (c) in the figure (2) using a commercial ellipsometer. The exchange energy between polaritonic modes is completely clear during incident angle variation upon the modal coupling spectra of cavities (a) and (b) unlike the cavity (c). Furthermore, the lower polaritonic mode located in the PL emission linewidth of Rubrene-like molecule so it exhibits less angle dependency compared to upper mode. On the other hand, there is an optimum EY51 film thickness that its luminescence can couple to both cavity and SPP modes within the plasmonc microcavities.

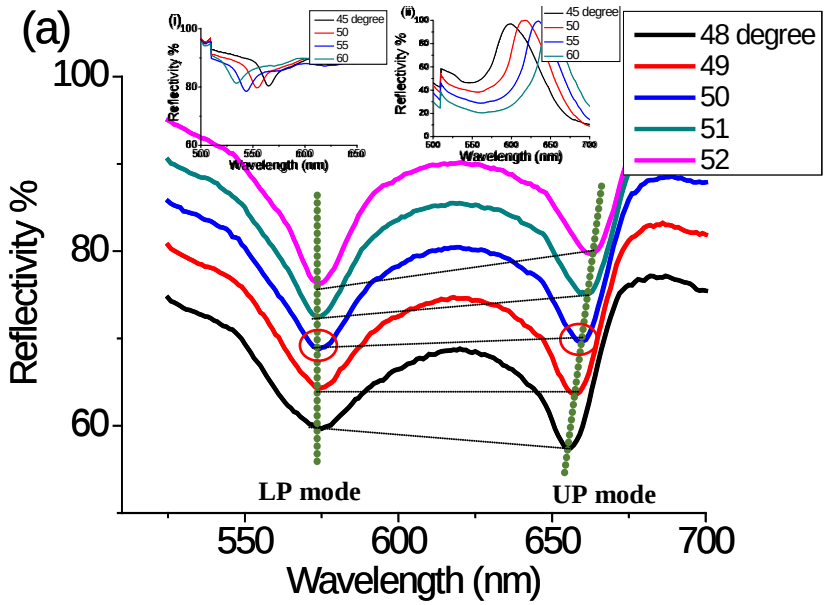
(a)
Reflectivity %
Wavelength (nm)
48 degree
49
50
51
52
LP mode
UP mode
(i)
(ii)
45 degree
50
55
60

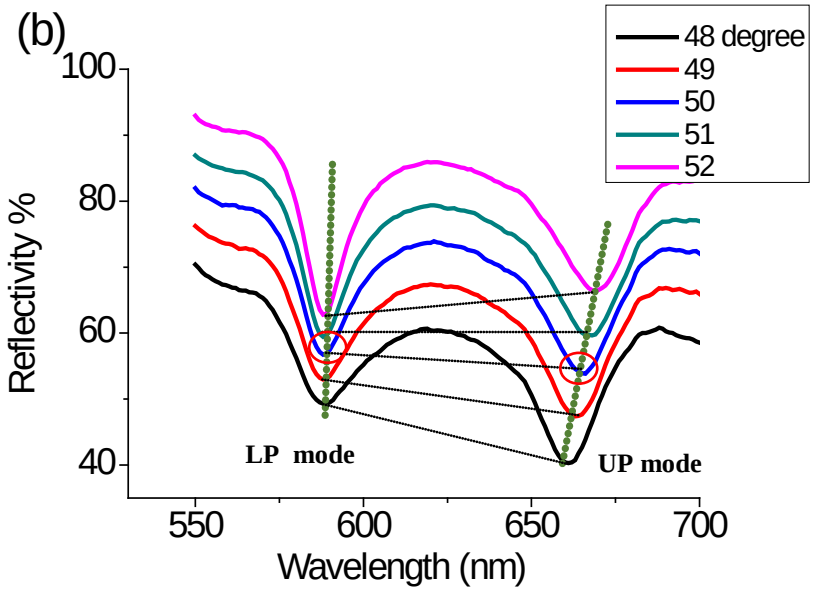
(b)
Reflectivity %
Wavelength (nm)
48 degree
49
50
51
52
LP mode
UP mode

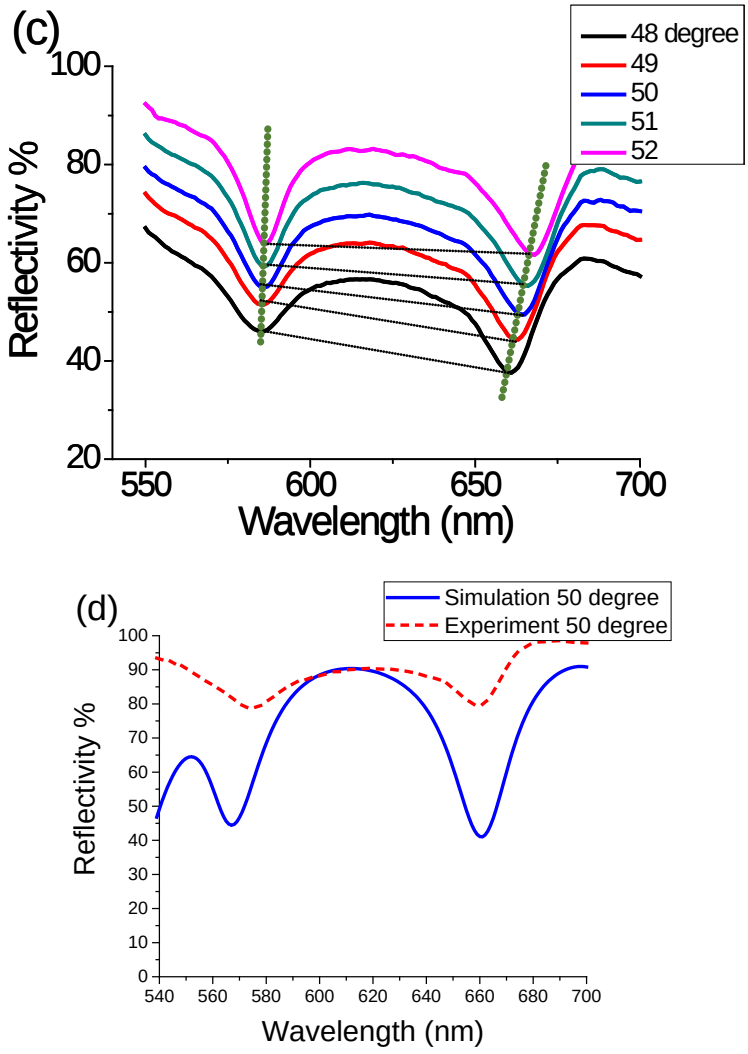

Figure 2. The Rabi-like splitting of strong modal coupling (a) the plasmonic micro cavity with 30nm EY51 layer. Rabi-like splitting is observed at 50 degrees; inset: (i) cavity mode and (ii) SPP mode , (b) the plasmonic microcavity with 50nm EY51 layer. Rabi-like splitting is observed at 50 degrees (c) there is no coupling for plasmonic microcavity with 80 nm EY51 layer. The coupling strength was measured in different incident angles; 48° to 52°, for cavity (a), (b) and (c). d) the simulation of strong coupling of cavity (b) which agrees with experimental spectrum.

The PL measurement was performed on plasmonic and photonic microcavity and the results are shown in figure (3a). The spectra show that there is a significant enhancement of PL intensity from the hybrid plasmonic microcavity, which means there is a potential in decreasing in pumping threshold of polariton lasers in the coupled system via large field enhancement inside the cavity. Besides, the photonic microcavity exhibits the cavity mode-exciton coupling with the Rabi-analogue splitting around the PL emission peak wavelength 538 nm; the splitting energy equals 240 meV (55 nm linewidth). The PL emission spectrum of EY51 on PMMA layer was shown in the figure (3b).

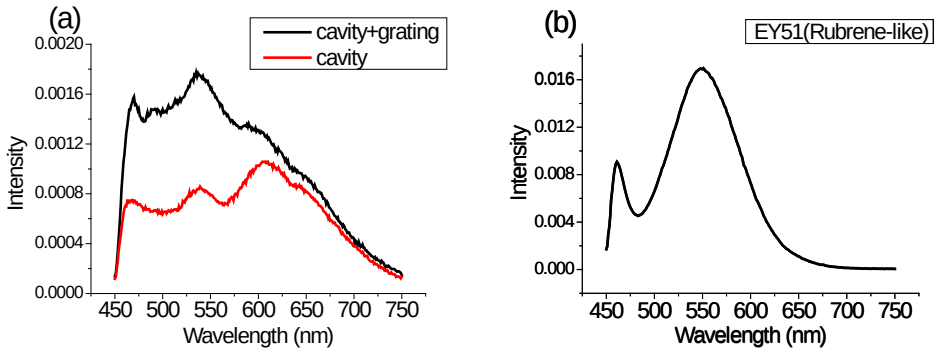

Figure 3. The PL emission from (a) the plasmonic and photonic microcavity, (b) EY51 thin film.

The PL emission involves a weak peak at the wavelength of 470 nm which is related to the emission of PMMA layer and also the PL emission of EY51 thin film on PMMA layer shows a blue shift rather than pristine Rubrene on the glass substrate due to the formation of some aggregations at the interface of molecules [10]. The result of Rubrene-like molecule-light interaction in the hybrid plasmonic microcavity promises novel opportunity to study modifiying molecular bonding and chemical landscape in next research works [11].

We now theoretically probe further on contribution from the active medium, EY51. Consider at the mode coupling point; then $\omega_{cav} = \omega_{spp} (= \omega_r)$. Then $\Delta\omega = 0,\ B = 0$ and

$A = 4g^2 - \Delta\Gamma^2$. Therefore the frequency shift (equation (2)) and the splitting ratio (equation (3)) become,

$$\omega_{\pm} = \frac{1}{2}\left[2\omega_r \pm \sqrt{A} + i\left(\Gamma_{cav} + \Gamma_{spp}\right)\right] \tag{4}$$

$$\gamma = \frac{2\sqrt{4g^2 - \Delta\Gamma^2}}{\Gamma_{cav} + \Gamma_{spp}} \tag{5}$$

At the coupling point, it is reasonable to assume that loss is minimum, thus, $g \gg \Delta\Gamma$. Simplying, $\sqrt{A} \approx 2g$, so equations (4) and (5) are reduced to,

$$\omega_{\pm} = \left[\omega_r \pm g + i\left(\frac{\Gamma_{cav} + \Gamma_{spp}}{2}\right)\right] \tag{6}$$

$$\gamma = \frac{\sqrt{8g}}{\Gamma_{cav} + \Gamma_{spp}} \tag{7}$$

Equations (6) and (7) can qualitatively support the mode coupling phenomena observed; the real part of equation (6) describes the mode frequency splits arising from the sum and difference of the resonant frequency with the coupling constant. The imaginary part describes the loss i.e. the inverse of Q factor; it should be at its minimum when the coupling is strongest. That means largest split i.e. γ is at its maximum. To achieve maximum γ, $(\Gamma_{cav} + \Gamma_{spp})$ in RHS of equation (7) is at its minimum; *g* is assumed to be a constant for a given coupled system. When the active medium is introduced into the microcavity, Γ_{cav} has changed and is due to EY51 absorbing the incident photons, converting them into emission that coupled to the SPP mode. This is evident by the increased in PL (Fig. 3a) when the cavity is coupled to the grating. This is further supported by the narrowing of linewidth of the resonant peaks (fig. 2b) (13 nm) at maximum PL/SPP coupling compare to that of minimum coupling (Fig. 2c) (17 nm). Note that the width of a resonance is inversely proportional to its

quality factor, which represents the net photon loss rate of the cavity. The presence of gain medium in any part of the cavity will increase the number of photons circulating in the cavity, as light traverses the gain medium will be amplified. Accordingly, the net photon loss rate of the cavity is reduced by the gain medium, because the introduction of the gain medium now generates additional photons. These physics are correct irrespective to the type of resonator or cavity, be it coupled or uncoupled. In fact, if we look at the route towards lasing, if we gradually increase the pump rate, the concerned resonance will first undergo spectrum narrowing before the pump rate is strong enough to induce lasing. Thus the presence of spectrum narrowing is a sign that the device was approaching lasing but not necessarily lasing. The above theoretical analysis shows that active medium enhance the Rabi-analogue split by suppressing the microacvity loss or acting as loss-compensation.

5. Conclusion

The large area plasmonic microcavity was fabricated with intermediate photoluminescence layer using the conventional laser interference lithography technique. The fabricated hybrid plasmonic device demonstrated the strong cavity mode-SPP coupling with a large Rabi-analogue splitting. The PL results for both plasmonic and photonic microcavity demonstrated increase in PL emission intensity in the hybrid plasmonic microcavity and the PL contributed to the mode coupling by suppressing the cavity loss. In this hybrid device, there is complex coupling within the microcavity in which the excitation energy generated coupling of two modes, SPP and cavity modes, with the PL from active medium acting as loss-compensation component. Therefore it is a form of parity time symmetry and further study is needed to investigate the physics within this complex coupling. The understanding will pave the way for many potential applications such as reduced threshold pumping of polariton lasers in future.

6. Acknowledgement

This work is supported by the Research Grant Council of Hong Kong under Projects AoE/P-02/12 and GRF grant 12303217.

[1] a) L. Novotny, B. Hecht, *Priciples of Nano-Optics*, Cambridge University Press, **2006**; b) R. Ameling, H. Giessen, *Nano Lett.* **2010**, *10*, 4394–4398; c) D. Chanda, K. Shigeta, T. Truong, E. Lui, A. Mihi, M. Schulmerich, P. V. Braun, R. Bhargava, J. A. Rogers, *Nat. Commun.* **2011**, *2*, 479 d) V. J. Sorger, R. F. Oulton, J. Yao, G. Bartal, X. Zhang, *Nano Lett.* **2009**, *9*, 10.

[2] a) R. Ameling, H. Giessen, *Laser Photonics Rev.* **2012**, 1–29; b) P. Törma, W. L. Barnes, *Rep. Prog. Phys.* **2015**, *78*.

[3] a) S. Kéna-Cohen, S. A. Maier, D. D. C. Bradley, *Adv. Optical Mater.* **2013**, *1*, 827-833; b) S. Chen, G. Li, D. Lei, K. W. Cheah, *Nanoscale* **2013**, *5*, 9129–9133; c) Z. Zhang, H. Wang, J. Du, X. Zhang, Y. Hao, Q. Chen, H. sun, *Applied Phys. Lett.* **2014**, *105*, 19; d) P. Chantharasupawang, L. Tetard, J. Thomas, *Phs. Chem. C* **2014**, *108*, 23954-23962.

[4] a) D. G. Lidzey, D. D. C. Bradley, M. S. Skolnick, T. Virgili, S. Walker, D. M. Whittaker, *Nature* **1998**, *395*, 6697, 53–55; b) R. J. Holmes, S. R. Forrest, *Org. Electron.* **2007**, *8*, 77–93.

[5] a) T. Virgili, L. Lüer, G. Cerullo, G. Lanzani, S. Stagira, D. Coles, A. J. H. M. Meijer, D. G. Lidzey, *Phys. Rev. B* **2010**, *81*, 125317; b) R. J. Holmes, S. R. Forrest, *Phys. Rev. Lett.* **2004**, *93*, 186404.

[6] a) P. Vasa, R. Pomraenke, G. Crimi, E. De Re, W. Wang, S. Schwieger, D. Leipold, E. Runge, G. Cerullo, C. Lienau, *ACS Nano* **2010**, *4*, 7559-7565; b) D. Melnikau, R. Esteban, D. Savateeva, A. Sánchez-Iglesias, M. Grzelczak, M. K. Schmidt, L. M. Liz-Marzán, J. Aizpurua, Y. P. Rakovich, *Phys. Chem. Let.* **2016**, *7*, 354-362; c) H. Wei, C. Jaing, Y. Chen, C. Lin, C. Cheng, C. Chan, C. Lee and J. Chang, *Opt. EXPRESS* **2013**, *21*, 21365-21373; d) F. Todisco, S. D'Agostino, M. Esposito, A. I. Ferna´ndez-Domı´nguez, M. De Giorgi, D. Ballarini, L. Dominici, I. Tarantini, M. Cuscuna´, F. D. Sala, G. Gigli, D. Sanvitto, *ACS Nano* **2015**, *9*, 10, 9691–9699.

[7] a) J. W. Menezes, J. Ferreira, M. J. L. Santos, L. Cescato, A. G. Brolo, *Adv. Funct. Mater.* **2010**, *20*, 3918–3924; b) A. C. R. Pipino, R. P. Van Duyne, G. C. Schatz, *Physical Rev. B* **1996**, *53*, 7, 4162.

[8] K. Ding, G. Ma, M. Xiao, Z. Q. Zhang, C. T. Chan, Phys. Rev. X **2016**, 6, 021007.

[9] F. H. Alast, G. Li, K. W. Cheah, *AIP Advances* **2017**, *7*, 085201.

[10] T. Iimori, R. Ito, N. Ohta, H. Nakano, *J. Phys. Chem. A* **2016**, 120, 4307-4313.

[11] T. W. Ebbesen, *Acc. Chem. Res.* **2016**, 49, 2403-2412.